Numerical investigation of displacement compatibility and interaction between reinforced concrete walls forming a system

Verdiana Miceli[1], Livio Pedone[1], Simone D'Amore[1], Michele Matteoni[1], Farhad Dashti[2], Patricio Quintana Gallo[3], Stefano Pampanin[1]

[1]Department of Structural and Geotechnical Engineering, Sapienza University of Rome, Via Eudossiana 18, 00184 Rome, Italy

[2]ZURU Tech HK Ltd, Tsim Sha Tsui, Hong Kong

[3]Department of Steel and Timber Structures, Czech Technical University in Prague, Thákurova 2077/7, 166 29 Prague 6, Prague, Czech Republic

Abstract

Previous research works pointed out that the displacement compatibility between walls of different lengths working in parallel may lead to a variation in seismic behaviour when compared to the same walls considered independently. Thus, as a part of a broader research project, this paper investigates the seismic behaviour of a system of two reinforced concrete walls of different lengths through a refined numerical model in DIANA. Results show that the shortest wall is characterised by a larger base shear and a smaller yielding displacement when analysed as part of the system rather than independently. Thus, neglecting the interaction between the system elements might lead to an unconservative estimation of shear demand in the shorter walls.

1 Introduction

Reinforced concrete (RC) structural walls have been widely adopted as primary lateral-force-resisting systems in earthquake-resistant structures. Typically, wall buildings are characterised by walls of different cross-section lengths [1]. Clearly, the length of a wall plays a crucial role in understanding its structural/seismic behaviour. More specifically, it is well known that the wall length is inversely proportional to the yielding curvature [2] and directly proportional to the flexural stiffness. Thus, walls with significantly different lengths are expected to have major differences in terms of these parameters. When these walls are combined to act within a system, the global as well as the individual response might be significantly affected by the interactions induced by displacement compatibility. Consequently, predicting the performance of walls when part of a system may be challenging, increasing the risk of an unreliable design process.

In the last decades, different studies have been conducted to understand the differences in the behaviour of walls when analysed independently or as part of a system. For instance, Paulay and Restrepo [2] analytically investigated a system of four RC walls with different lengths and same heights subjected to unidirectional monotonic lateral load. The authors suggested that the shear-displacement response (pushover curve) of the systems can be evaluated as the sum in parallel of the shear-displacement curves of the individual walls considered independently from each other. Later, Rutenberg and Leibovich [3] and Beyer et al. [4] studied a system of two walls linked together through infinitely rigid pin-ended connections. It was observed that the stiffest wall imposed its deformed shape on the shortest wall and that a redistribution of base shear occurred. More specifically, when compared to the seismic response of the individual walls considered independently, the shorter wall showed an increase in the base shear demand, whereas a decrease for the same parameter was observed for the longer wall. More recently, Quintana Gallo et al. [1] studied the pushover response of four slender cantilever rectangular RC walls of different lengths analysed both independently and as part of a system (i.e., considering displacement compatibility at each level imposed through cast-in-situ slabs). The authors numerically investigated the differences between the two analysed cases in terms of yielding top displacements, base shear demand and ultimate top displacement. The results showed that the shortest walls were characterised by

smaller yielding displacement, larger base shear and smaller ultimate displacement when analysed as part of a system rather than independently.

In line with and extending the research work of Quintana Gallo et al. [1], this paper aims at numerically investigating the differences in the seismic response of two RC walls when analysed independently or as part of a system. In the latter case, the walls are linked together in a parallel configuration through rigid pin-pin connections, which allow for displacement compatibility to be imposed at each level. The paper is structured as follows: in Section 2, a description of the case-study wall system is reported, while in Section 3 the adopted modelling approach is discussed. The results of nonlinear quasi-static analyses (both considering a unidirectional monotonic load and reversed-cyclic loads) are presented in Section 4. Finally, conclusions are given in Section 5.

2 Description of the case-study wall system

The study is implemented considering a system of two walls, namely "W1" and "W2" (Fig. 1, left), designed according to the Chilean Standard NCh433 [5] by Quintana Gallo et al. within a broader research project involving experimental testing (see the Acknowledgements section). These walls are characterized by the same height and width (h_w = 4000 mm, and e_w = 150 mm, respectively), but significantly different cross-section lengths (l_w), equal to 1500 mm and 300 mm for walls W1 and W2, respectively. Fig. 1 (right) shows the geometrical details of the walls' cross-sections.

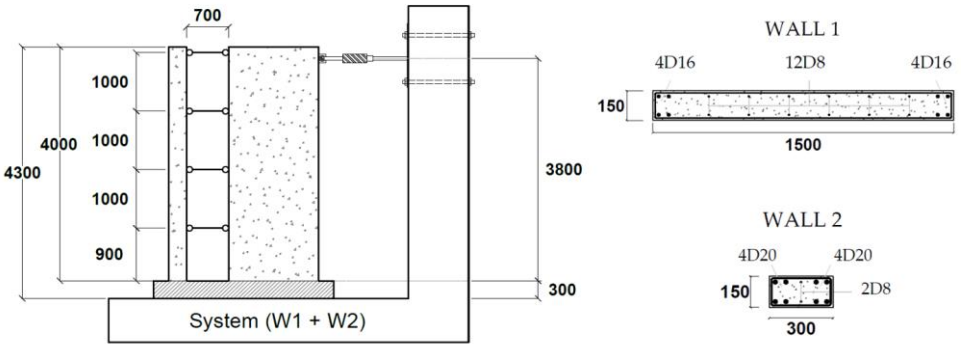

Fig. 1 (left) Longitudinal view of the wall system with detail of pin-pin connections; (right) cross-section of the two walls (D = diameter of reinforcement bars)

As longitudinal reinforcement, wall W1 has eight deformed bars D16 (16-mm-diameter bars) plus 12 deformed bars D8 spaced at 200 mm on-centre (o. c.), whereas wall W2 has four D20 plus two D8 bars (see Fig. 1). As horizontal rebar, in turn, W1 has D10 bars at 200 mm, whilst W2 has closed stirrups D8 spaced at 200 mm, which can provide some level of concrete confinement. Wall W1 does not have any confinement in the boundary zones. Moreover, the geometrical ratio of reinforcement (ρ_{cc}) is equal to 0.02 for the longest wall and to 0.07 for the shortest wall. Regarding the mechanical properties of the construction materials, the characteristic value of the compressive strength of the concrete is taken as $f_{ck} = 25\ MPa$, whereas a steel grade Gr60 was selected (yielding and ultimate stresses f_y = 420 MPa and f_u = 630 MPa, respectively). The height of the loading point corresponds to the height of the actuator and is equal to 3800 mm (Fig. 1, left).

3 Modelling approach

For each analysed configuration (i.e., RC walls considered either independently or forming a system), a refined numerical modelling approach, previously calibrated and verified against test results of walls with different failure modes [8], is used. The numerical simulation is conducted using DIANA FEA and with curved shell elements for modelling the wall components [6]. Specifically, CQ40S elements, i.e., quadrilateral eight-node isoparametric curved shell elements, are adopted. These second-order finite elements are chosen to capture geometric nonlinearities. Curved shell elements allow for reinforcing bars to be embedded to represent a perfect bond between concrete and steel. For the sake of simplicity, foundations are not explicitly modelled, thus the effects of wall-to-foundation interaction such as strain penetration or bond-slip of longitudinal reinforcement are herein neglected. Out-of-plane

displacements are restrained at each floor level as well as at the loading height. When part of a system, walls are linked in a parallel configuration through pin-pin connections that are modelled with a two-node translation spring identified as SP2TR in DIANA.

Regarding the applied loads, both dead weight and an imposed displacement history are considered in the model. For this type of analysis, the software DIANA requires defining a restrain for the translation in the applied deformation direction. Hence, translational supports acting in the global X direction (Fig. 2) are considered. It should be specified that the displacement is applied on top of each wall when analysed independently, as shown in Fig. 2 (left). On the contrary, when the walls are analysed interconnectedly, the displacement is applied on top of wall W1 only, (Fig. 2, right). In addition, to avoid stress localisation and ensure that the loads are properly spread across the walls, the top parts of the walls are modelled as an elastic material. Finally, geometric nonlinearities are also considered.

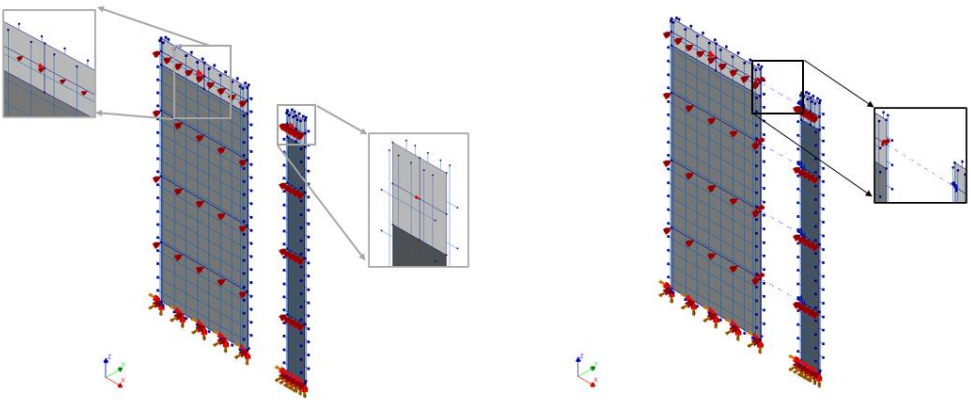

Fig. 2 Isometric view: (left) independent-case model with details of displacement applied on both walls and (right) system-case model with the detail of the spring connection.

More details on the adopted material properties and constitutive laws, as well as on the loading protocol, are given in the following paragraphs.

3.1 Material properties and constitutive laws

Concerning the material properties, the behaviour of concrete is modelled through the *total strain crack model*. This model is based on the Modified Compression Field Theory, proposed by Vecchio and Collins [7], and used in the model in the form of the *total strain rotating crack model*. The latter allows the orientation of the crack to rotate with the axes of principal strains (see, e.g., Dashti et al. [8]). The *total strain rotating crack model* is used for confined, unconfined, and elastic concrete. The difference between the three cases lies in how the tensile and compressive behaviour are described.

For concrete with elastic properties, adopted to model only the zones where the imposed displacement is applied, the *elastic* option is selected and the parameters are set as E_c = 28723 MPa and ν = 0.3, where E_c is Young's modulus (evaluated according to NTC2018 [9]) and ν is the Poisson ratio.

For the confined and unconfined concrete, the compressive behaviour is modelled according to the model proposed by Mander et al. [7], while the tensile behaviour is modelled according to Belarbi and Hsu [11]. The mean concrete compressive strength value (f'_{cm0} = 33 MPa, per NTC2018 [9]) rather than the characteristic value (f_{ck}) is considered in the model. The stress-strain curves are implemented through the *multilinear* option. Specifically, two different stress-strain curves were input to take into account the confinement of the shortest wall in the 2D model: one for the unconfined concrete (i.e., W1) and one for the confined concrete (i.e., W2). The values of the compressive strength and the ultimate strain of the latter depend on the geometrical ratio of transverse reinforcement (ρ_{st} = 0.006)

The ultimate strain of confined concrete, ε_{cu} =0.71%, is obtained with the formulation proposed by Priestley et al. [12], assuming an ultimate strain of transverse reinforcement equal to 3%. Moreover, the compressive strength of confined concrete (f_{cc}) is equal to 34 MPa and the corresponding strain (ε_{cc})

is equal to 0.23%. As mentioned before, the compressive strength of the unconfined concrete (f_{c0}) is equal to 33 MPa and the corresponding strain is equal to 0. 20%. A falling linear branch and an ultimate strain of 0.6% are considered in the model. For the concrete in tension, the tensile strength (f_{cr}) is equal to 1.8 MPa and the average tensile strain at the onset of concrete cracking (ε_{cr}) is equal to 0.008%.

The Menegotto-Pinto stress-strain relationship [13] is adopted for reinforcement steel bars. Yielding and ultimate stresses are set equal to 420 MPa and 630 MPa, respectively. The strain at the onset of strain hardening is 1%, whereas the strain at ultimate stress is 7%. Young's modulus (Es) is equal to 200 GPa. The parameters of the Menegotto-Pinto stress-strain relationship are selected according to the formulation proposed by Filippou et al. [14]. The latter is preferred as it accounts for the effect of isotropic hardening, which allows for a reduction of convergence issues in nonlinear analyses. Specifically, the required parameters are set as follows: R0 =20, b = 0.0154, a1= 18.5, a2=0.15, a3=0.01, a4=7. The parameter R0 accounts for the Bauschinger effect; a1 and a2 are the isotropic hardening parameters defining stress shift in compression; and a3 and a4 are the isotropic hardening parameters defining stress shift in tension [15]. Finally, spring connections are modelled with linear elastic behaviour and have an axial stiffness equal to 10^6 MPa, which allows for rigid-link functioning.

3.2 Nonlinear quasi-static analysis settings

Nonlinear quasi-static analyses are carried out considering either a unidirectional monotonic lateral load or reversed-cyclic loads. In the former protocol (i.e., monotonic analyses), the system is pushed to a maximum displacement of 120 mm (or an equivalent drift value of 3.15%), while in the latter protocol (i.e., reversed-cyclic analyses), the system is subjected to the loading history shown in Fig. 3. The convergence criteria are set in terms of force norm ratio (10^{-3}) and energy norm ratio (10^{-4}) [6], and the selected equilibrium iteration method is the S*ecant (Quasi-Newton)*.

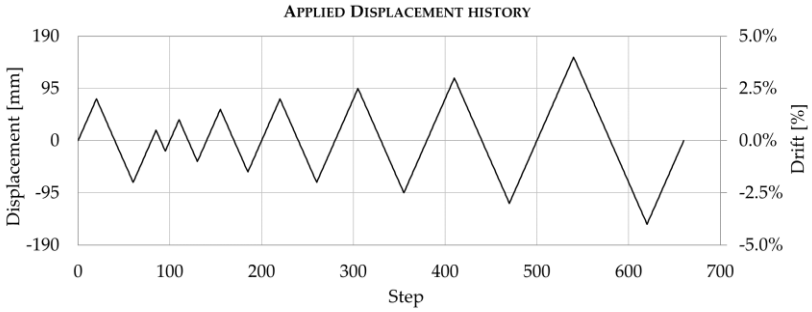

Fig. 3 Loading history for reversed-cyclic analyses

4 Results and discussion

4.1 Monotonic quasi-static analyses

The results of the monotonic quasi-static (pushover) analyses are presented in Fig. 4.

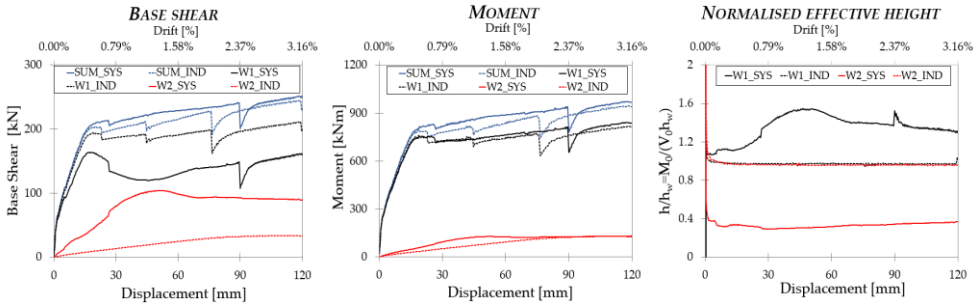

Fig. 4 Results of quasi-static monotonic analyses: (left) base shear vs. displacement; (centre) moment vs. displacement; (right) normalised effective height vs. displacement.

As shown in Fig. 4 (left), when considering the walls as a part of a system, a redistribution of the walls' base shear occurs. Specifically, when analysed as part of a system (_SYS) rather than independently (_IND), the longest wall,W1, shows a maximum base shear that is 1.2 times smaller whereas the shortest wall, W2, shows a maximum base shear that is 3 times bigger. It should be specified that the ratios, referred to the maximum base shear, change at different stages of loading. In turn, the total base shear of the system behaviour (SUM_SYS) is only slightly larger than the sum of the base shear of each wall treated independently (SUM_IND).

The shortest wall, W2, is characterised by a smaller yielding displacement when analysed as part of a system (42 mm) rather than independently (76 mm). On the contrary, W1 shows a slight increase in the yielding displacement. Neither the shortest, W2, nor the longest wall, W1, show a significant variation in terms of maximum moment demand when analysed as part of a system rather than independently (Fig. 4, centre). Moreover, similarly to the base shear, the total moment resisted by the walls for the system case is only slightly larger (3%) than the sum of the moment of the walls treated independently. This is an expected result, because the flexural strength of the walls is not affected by the system effect.

In addition, the normalised effective height is shown in Fig. 4 (right). In the independent case, both walls show a constant value of around 0.95, which is consistent with a loading point height of 3.8 m and a wall height of 4.0 m. Yet, when considered as part of a system, W1 shows an initial increase in the values of the normalised effective height, followed by a plateau and then a decrease with a mean value of 1.36. On the contrary, W2 shows an almost-constant trend with a mean value of around 0.33.

The results in terms of cracking pattern for three different values of drift (1%, 2%, and 3%) are also shown in Fig. 5, for the independent and system cases.

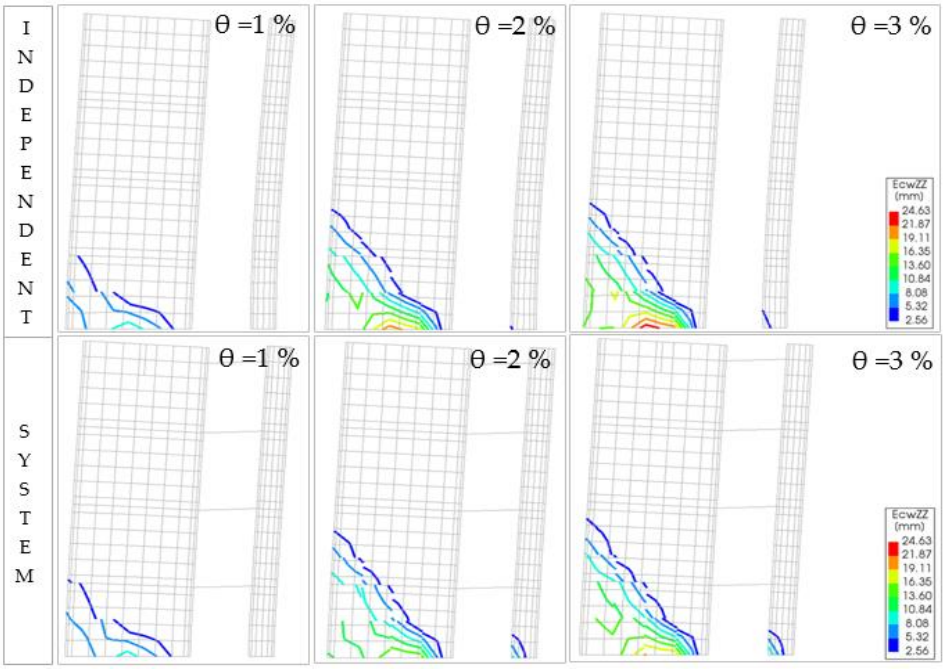

Fig. 5 Comparison between the cracking pattern of the walls when analysed independently and as part of a system at three different drift levels.

At a fixed drift value of 1%, only the longest wall yields for both the independent and system configurations. The observed orientation of the cracks would suggest a shear-dominated flexural-shear failure. Considering a higher drift of 2%, both walls have already yielded and shown cracks. In both the independent and system cases, the observed cracks at the base of W1 are less inclined and wider than cracks at the mid-height portion of the wall. When examined as part of a system, W2 is characterised by wider

and more inclined cracks compared to when analysed independently. This result is deemed due to the longest wall imposing its deformed shape on the shortest wall through rigid-link-functioning connections. Finally, the cracking pattern at the next step (i.e., drift value equal to 3%) is similar to the previous one. However, cracks are wider since a higher deformation demand is imposed on the walls and, as a consequence, the level of damage increases.

4.2 Quasi-static cyclic analyses

The results of the quasi-static cyclic analyses are reported in Fig. 6. It can be noted that stable and symmetrical cycles are observed both in tension and compression for each analysed configuration. The observed cyclic behaviour suggests that the analysed configurations are characterized by a great dissipation capacity.

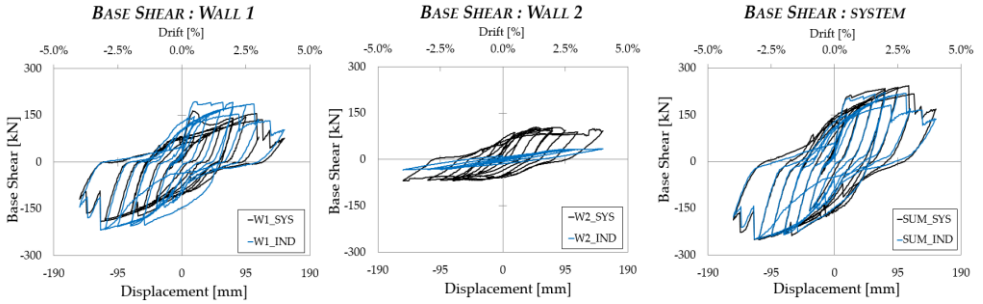

Fig. 6 Cyclic responses of: (left) W1 and (centre) W2 when considered either independently or as part of a system; (right) the wall system and the sum of the walls when analysed independently.

Results in terms of variation for the yielding displacement, base shear, base moment, and dissipated energy are listed in Table 1. In the initial part of the response (from values of 0% to 2% of the imposed drift), both cyclic and monotonic analyses show similar results. In fact, the same redistribution of base shear occurs, and the observed system total base shear is larger than the sum of the base shear of each wall (when considered independently). In addition, W2 shows a value of dissipated energy that is nine times greater when analysed as part of a system rather than independently. This result is due to the fact that, when part of a system, W2 has a much smaller yielding displacement, which increases its inelastic deformation, and it is also subjected to a higher base shear demand. Moreover, it is worth mentioning that W2 is characterised by significant ductility capacity and thus can undergo considerable inelastic deformations. This phenomenon is also deemed the reason why the cycles in the system case are larger than the cycles obtained as the sum of the base shear of the independent walls. Furthermore, it should be emphasised that the response of the shortest wall becomes asymmetric in the system case. As pointed out by Quintana Gallo and Dashti [16] this behaviour is due to the existence of static/sustained shear forces acting in the direction of analysis when the walls are interconnected.

Table 1 Observed values and percentage variation of yielding displacement (Δ_y), base shear (V_b), moment (M_b), and dissipated energy (E_{diss}) in the system case (SYS) compared to the independent case (IND) for the reversed-cyclic analyses

		V_b kN	SYS/IND variation	M_b kN	SYS/IND variation	E_{Diss} kNmm	SYS/IND variation
W1	IND	193.4	-15%	752.3	9%	173048.8	-11%
	SYS	163.9		819.5		153686.6	
W1	IND	34.4	203%	130.8	4%	8404.4	803%
	SYS	104.5		135.6		75917.3	
SUM	IND	222.1	10%	858.3	10%	181453.2	27%
	SYS	243.5		946.4		229603.9	

5 Conclusions

This paper presented a numerical investigation of the variation of the seismic behaviour of two RC walls when treated both independently or as part of a system. The study aims to extend the state-of-the-art works available in the literature on this topic, which have pointed out that significant differences in terms of yielding displacement and base shear take place when analysing walls with different lengths as part of an interconnected system rather than independently. In particular, the results of the numerical investigation provide a blind prediction of the upcoming experimental research part of a broader jointed research project funded by funded by ANID in Chile

To this end, a system of two RC walls of very dissimilar lengths has been analysed through a refined finite element model constructed in the software DIANA. Nonlinear quasi-static analyses were carried out considering monotonic and reversed-cyclic lateral displacement histories imposed at the top of the walls. The main conclusions can be summarised as follows:

- Consistently with previous results available in the literature, a redistribution of base shear and a variation of the yielding displacement was observed for both walls when analysed interconnectedly or independently;
- If analysed as part of a system rather than independently, the shortest wall presented a yielding displacement 0.6 times smaller and a 3-times-bigger base shear;
- As a consequence of the smaller yielding displacement, the shortest wall dissipates more energy during its response in the system case compared to the independent case (around 9 times bigger). Thus, the system shows larger ductility demand;
- The results in terms of total base shear and total base moment of the system were found to be slightly larger than the sum of the base shear and moment of each wall treated independently.

In conclusion, the seismic interaction between walls forming a system due to displacement compatibility issues should be taken into account in the design and assessment process. In fact, the results of this study have highlighted that neglecting the system effects could lead to an unreliable prediction of the seismic behaviour of the RC walls as well as to an unconservative estimation of the shear demand, particularly for the shortest walls. Future developments would involve experimental investigations to validate the results presented in this paper.

6 Acknowledgements

This work is aimed at providing a preliminary blind prediction of the results of the project “Experimental evaluation of the shear demand and the displacement capacity of reinforced concrete walls of different length forming a system” (contract FOVI210062), funded by ANID (Agencia Nacional de Investigación y Desarrollo), Chile. The authors want to acknowledge the financial support of the Italian Ministry of University and Research (MUR) for funding the Doctoral Scholarship of Michele Matteoni and Simone D’Amore. Livio Pedone received funding (post-doctoral research fellowship) from the ENHANCE research project.

7 References

[1] Quintana Gallo, Patricio, Farhad Dashti, Martín Caballero, and Rocío Álvarez. 2022.“Shear demand and inelastic displacement capacity of RC walls of different lengths forming a structural system.” *Bulletin of Earthquake Engineering* 20, 7315–7346. https://doi.org/10.1007/s10518-022-01494-w

[2] Paulay, Tom, and José I. Restrepo.1998. “Displacement and ductility compatibility in buildings with mixed structural systems.” *Journal of Structural Engineering Society New Zealand* 11:7-12.

[3] Rutenberg, Avigdor, and Edward Leibovich. 2002. “On the lateral force distribution among structural walls in multistorey buildings.” *Bulletin of the New Zealand Society for Earthquake Engineering* 35(4) 231–242. https://doi.org/10.5459/bnzsee.35.4.231-242

[4] Beyer, Katrin, Sabrina Simonini, Raluca Constantin, and Avigdor Rutenberg. 2014. “Seismic shear distribution among interconnected cantilever walls of different lengths.” *Earthquake Engineering and Structural Dynamics* 43:1423-1441. https://doi.org/10.1002/eqe.2403

[5] Instituto Nacional de Normalización (INN). 2012. *NCh433Of.96mod2012: Seismic design of buildings* (in Spanish)

[6] TNO. (2019). "DIANA finite element analysis user's manual: Release 10.3", Netherlands

[7] Vecchio, Frank J., and Michael P. Collins. 1986. "The Modified Compression Field Theory for Reinforced Concrete subjected to Shear". *ACI Journal*, Proceedings V. 83, No. 2.

[8] Dashti, Farhad, Rajesh P. Dhakal, and Stefano Pampanin. 2017. "Numerical Modelling of Rectangular Reinforced of planar RC walls". *Journal of Structural Engineering* 143(6) https://doi.org/10.1061/(ASCE)ST.1943-541X.0001729

[9] Ministero delle Infrastrutture e dei Trasporti. 2018."Norme tecniche per le costruzioni", *Gazzetta Ufficiale della Repubblica Italiana*, 20 February.

[10] Mander, John B., Michael J.N. Priestley, and Robert Park. 1988. "Theoretical stress-strain model for confined concrete ". *Journal of Structural Engineering* 144:1804 – 1826.

[11] Belarbi, Abdeldjelil, and Thomas T.C. Hsu. 1996. "Constitute Law of Reinforced Concrete Membrane Elements". Paper No. 1208 presented at the Eleventh World Conference on Earthquake Engineering, Acapulco, Mexico, June 23-28.

[12] Priestley, Michael J.N., Gian Michele Calvi, and Mervyn Kowalsky. 2007.*Displacement-based seismic design of structures*. Pavia: IUSS Press

[13] Menegotto, Marco, and Paolo E. Pinto.1973. "Method of analysis for cyclically loaded R.C. plane frames including changes in geometry and non-elastic behaviour of elements under combined normal force and bending". Proceedings of IABSE Symposium on Resistance and Ultimate Deformability of Structures Acted on by Well Defined Repeated Loads, 11:15-22

[14] Filippou, Filip C., Egor P. Popov, and Vitelmo V. Bertero. 1983. *Effects of bond deterioration on hysteretic behaviour of reinforced concrete joints*. Earthquake Engineering Research Center, Report No. UCB/EERC-83/19

[15] Carreno Vallejos, Rodrigo. 2018. *Characterization of Large Diameter Reinforcement Under Large Strain Cyclic Reversals*. PhD diss., UC San Diego

[16] Quintana Gallo, Patricio, and Farhad Dashti. 2023. "Estimating the yielding displacement and shear demand of a slender cantilever reinforced concrete wall including system and cyclic effects". Society for Earthquake and Civil Engineering Dynamics (UK) 2023 Conference, Cambridge, UK.